

Rapid Communication

## Production, purification and preliminary X-ray crystallographic studies of adeno-associated virus serotype 4

Nikola Kaludov,<sup>a</sup> Eric Padron,<sup>b</sup> Lakshmanan Govindasamy,<sup>b</sup> Robert McKenna,<sup>b</sup> John A. Chiorini,<sup>a,\*</sup> and Mavis Agbandje-McKenna<sup>b,\*</sup>

<sup>a</sup> GTTB, NIDCR, National Institutes of Health, Bethesda, MD 20892, USA

<sup>b</sup> Department of Biochemistry and Molecular Biology, Center for Structural Biology, The McKnight Brain Institute, College of Medicine, University of Florida, Gainesville, FL 32610, USA

Received 19 August 2002; returned to author for revision 27 September 2002; accepted 2 October 2002

### Abstract

Adeno-associated virus (AAV) serotypes 1 to 5 are currently under development as clinical gene delivery vectors for the treatment of human diseases. However, the ubiquitous nature of their cell surface receptors, heparin sulfate (AAV2 and 3) and sialic acids (AAV4 and 5), can preclude specific tissue targeting *in vivo*. Structural studies of AAV4 were initiated to characterize its capsid surface for re-targeting manipulations. Crystals obtained diffracted synchrotron radiation to 3.2 Å resolution. The unit cell is body-centered orthorhombic, I222, with  $a = 339.6$ ,  $b = 319.2$  and  $c = 285.0$  Å. The virus particle orientation and position have been determined.

© 2003 Elsevier Science (USA). All rights reserved.

**Keywords:** Adeno-associated virus; Gene therapy; Parvovirus; Crystallization; Virus structure

### Introduction

The five distinct serotypes of adeno-associated viruses (AAV1 to AAV5), members of the *Parvoviridae* family, are helper dependent parvoviruses (Muzyczka and Berta, 2001). The past few years have seen rapid progress in the development of the AAV serotypes for gene therapy applications. They are non-pathogenic, non-toxic and can package and deliver foreign genes to target cells. However, it is becoming evident that the different serotypes have unique cellular binding characteristics (Kaludov et al., 2001; Walters et al., 2002; Rabinowitz et al., 2002) despite the fairly high sequence homology between their capsid sequences. AAV2 and AAV3 that are ~87% identical utilize heparin sulfate as their primary receptor (Summerford and Samulski, 1998; Handa et al., 2000), but with different binding affinities (Rabinowitz et al.,

2002). AAV1 that is ~83% identical to AAV2 does not bind heparin sulfate (Rabinowitz et al., 2002). AAV4 and AAV5 that are ~55% identical to AAV2 and to each other bind sialic acid, not heparin sulfate (Davidson et al., 2000; Rabinowitz et al., 2002). Recently it was shown that AAV4 binds  $\alpha 2,3$  O-linked sialic acids, while AAV5 binds both  $\alpha 2-3$  and  $\alpha 2-6$  N-linked sialic acids (Kaludov et al., 2001; Walters et al., 2002). These tropism differences and the desire to improve AAV gene therapy applications have generated significant interest in the capsid structure of the different serotypes (Xie et al., 2002). This paper reports the production, purification and preliminary X-ray crystallographic studies of AAV4. The determination of the atomic structure of AAV4 is critical for fully elucidating its functional domains as it relates to receptor binding and antigenic properties. Understanding these architectural designs will maximize its exploitation for gene therapy applications.

### Results and discussion

#### *Virus production, purification and crystallization*

Wild-type AAV4 particles were produced in Cos cells and purified using a CsCl density gradient and centri-prep

\* Corresponding author. Department of Biochemistry and Molecular Biology, Center for Structural Biology, The McKnight Brain Institute, College of Medicine, University of Florida, Gainesville, FL 32610-0245. Fax: +1-352-392-3422; E-mail: [mckenna@ufl.edu](mailto:mckenna@ufl.edu) (MAM) and GTTB, NIDCR, National Institutes of Health, Bethesda, MD 20892. Fax: +1-301-402-1228.

E-mail address: [jchiorini@dir.nidcr.nih.gov](mailto:jchiorini@dir.nidcr.nih.gov) (J.A. Chiorini).

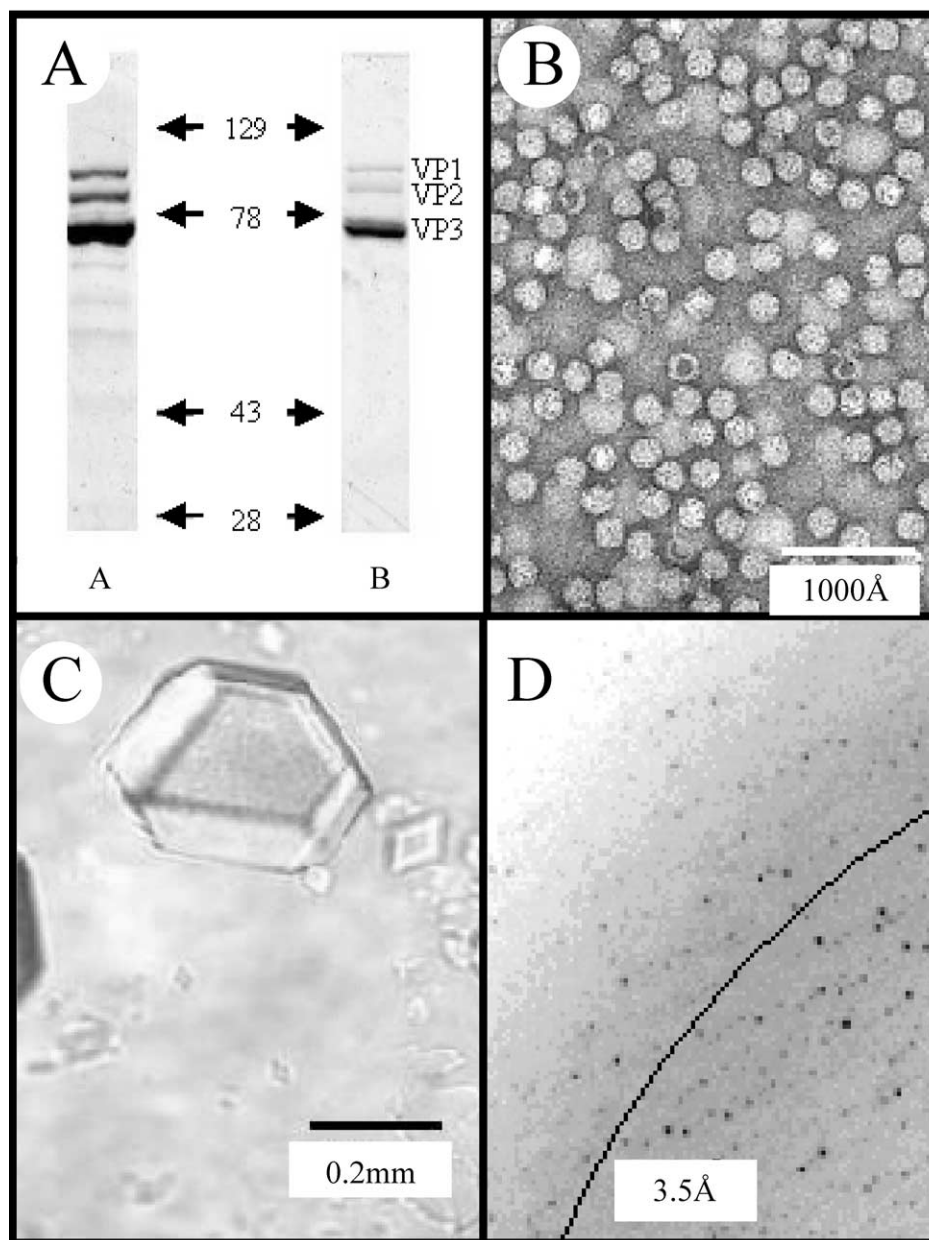


Fig. 1. AAV4 production, purification and X-ray diffraction data. A) SDS-PAGE of purified wild-type AAV4 particles. The number of purified DNase resistant genomes was calculated by QPCR. Lane A shows  $5 \times 10^{11}$  particles from the CsCl gradient fractions and Lane B shows  $2 \times 10^{11}$  particles from the final purification step, resuspended in SDS sample buffer and separated on a 4–21% polyacrylamide gel. The gel was stained with SyproRed and visualized using storm 860. The positions of molecular weight standards and the three AAV4 coat proteins are indicated. B) An electron micrograph of purified AAV4 particles stained with 2% uranyl acetate and applied to a 400 mesh carbon coated cooper grid. The micrograph was taken with a Joel JEM-100CX II electron microscope at a magnification of 40,000 $\times$ . The magnification bar represents 1000 Å. C) An optical photograph of the AAV4 crystals in a hanging drop, taken with a Zeiss Axioplan 2 microscope. The approximate dimensions of the crystals are  $0.2 \times 0.2 \times 0.2$  mm. D) A magnified portion of a typical  $0.25^\circ$  oscillation photograph for an AAV4 crystal diffracting X-rays to 3.2 Å resolution. The image was collected on an ADSC Quantum4 CCD detector at the F1 beam line ( $\lambda = 0.916$  Å) at the Cornell High Energy Synchrotron Source with an exposure time of 90s and a crystal to detector distance of 300 mm. The black curved line shows the demarcation of the 3.5 Å resolution diffraction shell.

filtration for structural studies by X-ray crystallography. Approximately  $1 \times 10^5$  DNase resistant particles/cell were obtainable in each preparation. SDS-PAGE (Fig. 1A) and negative stain electron microscopy (Fig. 1B) confirmed the purity and quality of the virus particles, respectively. The

amount of sample obtained after purification was adequate for crystallization experiments.

Small diamond-like crystals, approximately  $0.2 \times 0.2 \times 0.2$  mm in size, were obtained in 4 to 8 weeks (Fig. 1C) from purified AAV4 samples. Good quality crystals suitable

Table 1  
Crystal data set statistics

Resolution shells (Å)	No. of unique reflections	Completeness (%)	$R_{\text{sym}}^*$
50.00 7.53	15111	75.8	0.085
7.53 5.98	16556	84.8	0.114
5.98 5.23	16594	85.5	0.132
5.23 4.75	16548	85.4	0.142
4.75 4.41	16565	85.8	0.156
4.41 4.15	16575	85.8	0.174
4.15 3.94	16559	85.8	0.200
3.94 3.77	16565	86.0	0.224
3.77 3.63	16477	85.6	0.252
3.63 3.50	16015	83.2	0.269
Total to 3.50	163565	84.3	0.159
3.5 3.31	18732	50.8	0.379
3.31 3.20	10703	42.6	0.426
Total to 3.20	186958	75.9	0.164

\*  $R_{\text{sym}}$  is defined as  $\sum(|I - \langle I \rangle| / \sum I)$ , where  $I$  is the intensity of an individual reflection and  $\langle I \rangle$  is the average intensity for this reflection; the summation is over all intensities.

for X-ray diffraction data collection were obtained using virus concentrations ranging from 2 to 4 mg/ml in 20 mM Tris-HCl, pH 7.5, with 2 mM MgCl<sub>2</sub>, 150 mM NaCl and 1–1.5% PEG8000.

#### Data collection and processing

Initial room temperature X-ray diffraction data collection tests at the F1 station at CHESS showed the AAV4 crystals to be ordered to at least 3.2 Å resolution. However, the crystals were highly sensitive to synchrotron radiation damage, with only 2–4 images being collected per crystal. To overcome this radiation sensitivity problem, a suitable cryo-protectant solution was developed. This solution contained the crystallization conditions, with the percentage of the PEG increased to 5%, plus 30% glycerol. During the data collection the frozen crystals still showed the effects of radiation damage (slow decay of X-ray diffraction pattern resolution and increased mosaicity) with prolonged exposure to X rays, although this was drastically reduced compared to room temperature data collection. A total of 276 images were collected from 6 frozen crystals (average of ~45 images each) that all diffracted X rays to at least 3.5 Å resolution; 4 of the crystals diffracted X rays to 3.2 Å resolution (Fig. 1D).

The intensity data were initially processed (Otwinowski & Minor, 1997) to 3.5 Å resolution with the orthorhombic crystal system I222 with unit cell parameters  $a = 339.6$ ,  $b = 319.2$ , and  $c = 285.0$  Å. The data set was merged to 163,565 independent reflections (84.3% complete overall and 83.2% complete in the outermost resolution shell), resulting in an  $R_{\text{sym}}$  of 15.9% (26.9% in the outermost resolution shell). The resolution of the processing was then extended to 3.2 Å to include the few higher resolution reflections, resulting in an  $R_{\text{sym}}$  of 16.4% (42.6% in the outermost resolution shell) for 192,100 merged independent

reflections (75.9% complete overall, 42.6% complete in the outermost resolution shell) (Table 1). The quality and percentage of data (Table 1) is comparable or better than those that have been used for the structure determination of other parvovirus capsids (e.g., Agbandje et al., 1993; Llamas-Saiz et al., 1997; Simpson et al., 2002), including AAV2 (Xie et al., 2002). The average reflection intensity ( $I$ ) to noise ( $\sigma(I)$ ) ratio,  $[I/\sigma(I)]$ , was 4.41 for data up to 3.2 Å resolution (Table 2).

The orthorhombic cell dimensions and the molecular weight of the AAV4 virus give a  $V_M$  (Matthews, 1968) value of 4.3, 2.2 and 1.1 Å<sup>3</sup>/Da for one, two, and four particle per unit cell, respectively. By comparison of  $V_M$  values for other virus crystals, the only reasonable value is two particles per unit cell with a solvent content of 41%, assuming a molecular density of 1.30 g/cm<sup>3</sup> (Table 2).

There are two possible body-centered orthorhombic space groups I222 and I2<sub>1</sub>2<sub>1</sub>2<sub>1</sub> (Henry and Lonsdale, 1969). On consideration of packing constraints for two particles in these space groups the most likely space group was I222, with both particles having the same orientation, with 3 mutually perpendicular twofold icosahedral symmetry axes coincident with the crystallographic twofold axes. Table 2 gives a summary of the data collection and crystal characterization results.

#### Determination of particle orientation and position

The orientations of the two AAV4 particles in the unit cell were determined with self-rotation functions (Rossmann and Blow, 1962). The function was explored searching for 5-, 3- and 2-fold icosahedral symmetry axes of the virus particles. The rotation function for  $\kappa = 72^\circ$  (to search for the fivefold non-crystallographic symmetry axes directions) is shown in Fig. 2a. The observed peaks were consistent with an orientated standard icosahedron, having three mutually perpendicular twofold axes parallel to the **a**, **b** and **c** unit cell axes (Fig. 2b). The rotation functions for

Table 2  
Summary of data collection parameters and crystal characterization<sup>#</sup>

Crystal dimensions (mm)	0.2 × 0.2 × 0.2
Temperature (K)	100
Wavelength (Å)	0.916
Resolution range (Å)	50–3.5 (3.2)
Crystal System	Orthorhombic
Space group	I222
Unit cell parameters (Å)	$a = 339.6$ $b = 319.2$ $c = 285.0$
Total number of reflections	3109095 (3500729)
No. of Unique reflections	163565 (192100)
$R_{\text{sym}}^*$	15.9 (16.4)
Completeness (%)	84.3 (75.9)
Average $I/\sigma(I)$	4.41
No. of particles	2
Solvent content (%)	41
$V_M$ (Å <sup>3</sup> /Da)	2.2

<sup>#</sup> Data statistics at 3.2 Å resolution are given in the parenthesis.

\*  $R_{\text{sym}}$  definition is as in Table 1.

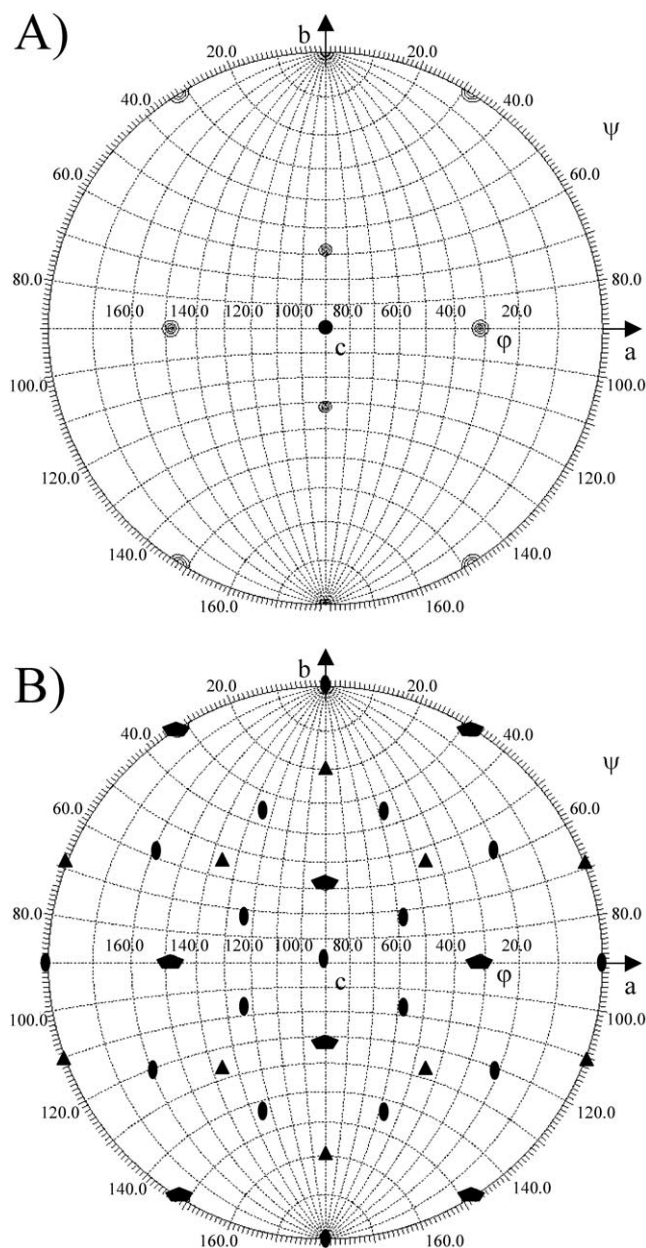


Fig. 2. Stereographic projections showing rotation function results for the AAV4 X-ray diffraction data. A) The rotation function for  $\kappa = 72^\circ$ , showing a search for fivefold icosahedral symmetry elements, using the observed data set in the 10 to 3.5 Å resolution range, with a radius of integration of 120 Å. The map is contoured at  $3\sigma$ . B) The definition of a standard icosahedral orientation, back solid pentagons, triangles and ellipsoids represent 5-, 3- and 2-fold symmetry axes, respectively. Three mutually perpendicular icosahedral twofold axes are parallel to the unit cell *a*, *b* and *c* axes.

$\kappa = 120^\circ$  and  $180^\circ$  were calculated and were consistent with this orientation (data not shown). The rotation function searches showed that the two virus particles in the unit cell have the same orientation (only one unique orientation was observed) and that the virus particles share twofold symmetry axes with the I222 space group.

Packing of the AAV4 particles in the I222 unit cell, with

their crystallographically constrained orientations, requires them to be situated at  $(0, 0, 0)$  and  $(\frac{1}{2}, \frac{1}{2}, \frac{1}{2})$ . This would allow the particles to have a maximum diameter of  $\sim 285$  Å. This is consistent with the diameter of parvovirus particles that are approximately 260 Å (Agbandje et al., 1995).

Initial phases for the AAV4 X-ray diffraction data has been calculated to 3.2 Å resolution using the CNS program (Brünger et al., 1998) from a poly-alanine feline panleukopenia virus (FPV) model (Agbandje et al., 1993) directly oriented and positioned in the I222 unit cell. This model resulted in an initial phasing  $R_{\text{factor}}$  of 47%, ( $R_{\text{factor}} = \frac{\sum(|F_{\text{obs}}| - |F_{\text{calc}}|)}{\sum|F_{\text{obs}}|}$ , where  $F_{\text{obs}}$  and  $F_{\text{calc}}$  represent the observed data and calculated (from the model) amplitudes, respectively). Thus, a molecular replacement model is at hand. Using 15-fold non-crystallographic symmetry to average the calculated electron density maps, the structure determination of AAV4 to 3.2 Å resolution should proceed without difficulties. This preliminary work represents a major step toward obtaining the essential high resolution structural data for AAV4 required for understanding the properties of its capsid and its manipulation for improved gene therapy applications.

## Materials and methods

### Production and purification

Cos cells used for viral production were maintained as monolayer cultures in D10 medium (Dulbecco's modified Eagle's medium containing 10% fetal calf serum, 100 U of penicillin per ml, 100 mg of streptomycin per ml, and 13 U amphotericin B as recommended by the manufacturer (GIBCO, Gaithersburg, MD). Wild-type AAV4 was produced in the Cos cells by infection with AAV4 (m.o.i. 100) and adenovirus type 5 (m.o.i. 10). The infected cells were harvested by scraping at 48 h post infection and virus was then purified and concentrated as described by Kaludov et al., 2001, with the following modifications. The virus was initially purified with a 1.4 g/cm<sup>3</sup> CsCl density gradient by centrifugation at 38 K for 65 h at 4°C. The semi-purified virus was concentrated on centri-prep 100 filters (Millipore) and washed with a 1% deoxycolic acid solution to remove contaminating proteins co-purified in the CsCl gradient. The virus was then washed with 20 mM Tris-HCl, pH 7.5, with 2 mM MgCl and 150 mM NaCl and re-concentrated to approximately  $3$  to  $4 \times 10^{14}$  particles/ml ( $\sim 3$ – $4$  mg/ml) using the centri-prep 100 filters. Viral titer was determined by QPCR as described by Kaludov et al., 2001. One microliter of purified virus was added to a PCR reaction containing 1X SYBR Green master mix (ABI, Foster City, CA), 0.25 pmol/ $\mu$ l forward and reverse primers and amplification was detected using an ABI 7700 sequence detector (ABI, Foster City, CA). Specific primers for AAV4 were designed by using the primer express program (ABI, Foster city, CA): Forward 5'-ACCAACATCGCGGAGGC, Reverse 5'-

CCCTCCTCCCACCAGATCA. Following a 96°C 10 min denaturing step, cycling conditions were 96°C for 15 s, 60°C for 1 min for 40 cycles. The viral DNA in each sample was quantified by comparing the fluorescence profiles with a set of DNA standards.

#### *Negative stain electron microscopy*

Purified AAV4 particles were viewed using a Joel JEM-100CX II electron microscope (EM) at a magnification of 40 K. Five microliters of purified virus, at an estimated concentration of 0.3 mg/ml, was spotted onto a 400 mesh carbon coated copper grid (Ted Pella, Inc., Redding, CA) for 1 min before blotting with filter paper (Whatman # 5). The sample was then negatively stained with 5  $\mu$ l of 2% uranyl acetate for 10 s, blotted dry and viewed with the EM.

#### *Crystallization*

Crystallization conditions were initially screened, based on previously reported conditions used for autonomous parvoviruses (Tsao et al., 1992; Agbandje et al., 1993; Llamas-Saiz et al., 1997), using hanging drop vapor diffusion (McPherson, 1982) in VDX 24 well plates and siliconized cover slips (Hampton Research, Laguna Niguel, CA). The conditions were further refined by searching virus concentration (2–4 mg/ml) and percentages (0.5–3%) of polyethylene glycol 8000 (PEG 8000). Crystallization drops contained 2  $\mu$ l of virus mixed with 2  $\mu$ l of precipitant solution consisting of 20 mM Tris–HCl, pH 7.5, with 2 mM MgCl<sub>2</sub>, 150 mM NaCl and PEG8000. The drops were equilibrated by vapor diffusion against 1 ml of precipitant solution at room temperature.

#### *X-ray diffraction data collection and processing*

All X-ray diffraction data were collected at the F1 beam line at the Cornell High energy Synchrotron Source (CHESS, Ithaca, NY), using an ADSC Quantum4 CCD detector system. The X-ray diffraction data collection was performed at cryo (~100 K) temperatures after initially testing the diffraction quality at room temperature. The crystals were transferred to a freshly prepared cryo protectant solution consisting of 30% glycerol in the precipitant solution (20 mM Tris–HCl, pH 7.5, with 2 mM MgCl<sub>2</sub>, 150 mM NaCl and PEG8000). The crystals were allowed to equilibrate for 5 min and then mounted on a thin fiber (0.2 mm) cryo-loop (Hampton Research) and transferred into a cryo stream (Oxford Cryosystems, Oxford, UK) for flash freezing. Data were collected at a wavelength of  $\lambda = 0.916$  Å with a 0.2 mm collimator and a crystal-to-detector distance of 300 mm. All images were collected using a 0.25° oscillation angle with exposure times ranging from 60 to 120 s per image.

The collected diffraction data were indexed using the software DENZO and scaled and reduced with SCALEPACK (Otwinowski and Minor, 1997).

#### *Determination of particle orientation and position*

The orientations of the virus particles in the crystal unit cell were determined with a self-rotation function (Rossmann and Blow, 1962) using the GLRF program (Tong and Rossmann, 1990). The self-rotation function calculation was computed using ~10% of the observed data between 10 to 3.5 Å resolution at kappa angles of 72° (fivefold), 120° (threefold) and 180° (twofold) with the radius of integration set to 120 Å. The particle position was inferred by packing considerations. The previously determined structure of FPV (Agbandje et al., 1993) was used as an initial phasing model. All the side chains were removed and fifteen copies of a poly-alanine capsid protein model were directly orientated and positioned in the I222 unit cell. The crystallographic symmetry operators were applied to generate the two complete icosahedral particles in the unit cell. The initial phases were then calculated from the model to 3.2 Å resolution using the CNS program (Brünger et al., 1998). All calculations were performed on an RS10000 computer (Silicon Graphics Inc., Orlando, FL).

#### **Acknowledgments**

We thank the MacCHESS staff for their help during X-ray diffraction data collection at the Cornell High Energy Synchrotron (CHESS) Facility, Ithaca, NY. We specially thank Lana Walsh at CHESS for help in obtaining beamtime (EM 407, 477). We also thank the McKenna lab members David Duda, Robbie Reutzler, and Craig Yoshioka for help during X-ray diffraction data collection at CHESS, and Beverly Handelman at the NIH (GTTB, NIDCR) for excellent technical assistance. We thank Dennifield Player (Anatomy and Cell Biology, University of Florida) for help with electron microscopy and Timothy Vaught (McKnight Brain Institute, Optical Microscopy facility, University of Florida) for taking the photograph of the AAV4 crystals. This project is funded in part by an internal College of Medicine Howard Hughes Medical Institute Biomedical Research Support Program for Medical Schools Pilot Project from the University of Florida (MAM).

#### **References**

- Agbandje, M., McKenna, R., Rossmann, M.G., Strassheim, M.L., Parrish, C.R., 1993. Structure determination of feline panleukopenia virus empty particles. *Proteins* 16, 155–171.
- Agbandje, M., Parrish, C.R., Rossmann, M.G., 1995. The structure of parvoviruses. *Sem. Virol.* 6, 299–309.
- Brünger, A.T., Adams, P.D., Clore, G.M., DeLano, W.L., Gros, P., Grosse-Kunstleve, R.W., Jiang, J.S., Kuszewski, J., Nilges, M., Pannu, N.S., Read, R.J., Rice, L.M., Simonson, T., Warren, G.L., 1998. Crystallography and NMR system: a new software suite for macromolecular structure determination. *Acta Cryst. D* 54, 905–921.
- Davidson, B.L., Stein, S.C., Heth, J.A., Martins, I., Kotin, R.M., Derksen, T.A., Zabner, J., Ghodsi, A., Chiorini, J.A., 2000. Recombinant adeno-associated virus type 2, 4, and 5 vectors: transduction of variant cell

- types and regions in the mammalian central nervous system. *Proc. Natl. Acad. Sci. USA* 97, 3428–3432.
- Handa, A., Muramatsu, S., Qiu, J., Mizukami, H., Brown, K.E., 2000. Adeno-associated virus (AAV)-3-based vectors transduce haematopoietic cells not susceptible to transduction with AAV-2-based vectors. *J. Gen. Virol.* 81, 2077–2084.
- Henry, N.F.M., Lonsdale, K., 1969. *International Tables for X-Ray Crystallography, Vol 1: Symmetry groups*. The Kynoch Press, Birmingham, England.
- Kaludov, N., Brown, K.E., Walters, R.W., Zabner, J., Chiorini, J.A., 2001. Adeno-associated virus serotype 4 (AAV4) and AAV5 both require sialic acid binding for hemagglutination and efficient transduction but differ in sialic acid linkage specificity. *J. Virol.* 75, 6884–6893.
- Llamas-Saiz, A.L., Agbandje-McKenna, M., Wikoff, W.R., Bratton, J., Tattersall, P., Rossmann, M.G., 1997. Structure determination of minute virus of mice. *Acta Cryst. D* 53, 93–102.
- Matthews, B.W., 1968. Solvent content of protein crystals. *J. Mol. Biol.* 33, 491–497.
- McPherson, A., 1982. *Preparation and analysis of protein crystals*, 1st Ed. Wiley & Sons, New York, pp. 96–99.
- Muzyczka, N., Berta, S.C., 2001. Parvoviridae: The viruses and their replication, in: Knipe, D.M., Howley, P.M. (Eds.), *Fields Virology*, 4th ed. Lippincott Williams and Wilkins, New York, pp. 2327–2360.
- Otwinowski, Z., Minor, W., 1997. In: Carter, C.W., Jr., Sweet, R.M. (Eds.), *Methods in Enzymology: Macromolecular Crystallography, Part A*, Vol. 276. Academic Press, London, pp. 307–326.
- Rabinowitz, J.E., Rolling, F., Li, C., Conrath, H., Xiao, W., Xiao, X., Samulski, R.J., 2002. Cross-packaging of a single adeno-associated virus (AAV) type 2 vector genome into multiple AAV serotypes enables transduction with broad specificity. *J. Virol.* 76, 791–801.
- Rossmann, M.G., Blow, D.M., 1962. The detection of sub-units within the crystallographic asymmetric unit. *Acta Cryst.* 15, 24–31.
- Simpson, A.A., Hébert, B., Sullivan, G.M., Parrish, C.R., Zádori, Z., Tijssen, P., Rossmann, M.G., 2002. The structure of the porcine parvovirus: comparison with related viruses. *J. Mol. Biol.* 315, 1189–1198.
- Summerford, C., Samulski, R.J., 1998. Membrane-associated heparin sulfate proteoglycan is a receptor for Adeno-associated virus type 2 virions. *J. Virol.* 72, 1438–1445.
- Tsao, J., Chapman, M.S., Wu, H., Agbandje-Mckenna, M., Keller, W., Rossmann, M.G., 1992. Structure determination of monoclinic canine parvovirus. *Acta Cryst. B* 48, 75–88.
- Tong, L., Rossmann, M.G., 1990. The locked rotation function. *Acta Cryst. A* 46, 783–792.
- Walters, R.W., Pilewski, J.M., Chiorini, J.A., Zabner, J., 2002. Secreted and transmembrane mucins inhibit gene transfer with AAV4 more efficiently than AAV5. *J. Biol. Chem.* 277, 23709–23713.
- Xie, Q., Bu, W., Bhatia, S., Hare, J., Somasundaram, T., Azzi, A., Chapman, M.S., 2002. The atomic structure of adeno-associated virus (AAV-2), a vector for human gene therapy. *Proc. Natl. Acad. Sci. USA* 99, 10405–10410.